

Article

Study of Rock Damage Constitutive Model Considering Temperature Effect Based on Weibull Distribution

Tianci Lu ¹, Hao Wu ¹, Shuiming Yin ¹ and Xiaoli Xu ^{1,2,*} 

¹ School of Transportation and Civil Engineering, Nantong University, Nantong 226000, China; 2233310012@stmail.ntu.edu.cn (T.L.); 2133110354@stmail.ntu.edu.cn (H.W.); 2333310007@stmail.ntu.edu.cn (S.Y.)

² Key Laboratory of Safety and High-Efficiency Coal Mining, Ministry of Education, Anhui University of Science and Technology, Huainan 232001, China

* Correspondence: xuxiaoli2002_ren@163.com

Abstract: The deformation and damage process of rocks is accompanied by crack extension and penetration. The rock strength criterion, as a macroscopic characterization of the rock strength microelement, is the basis for establishing the damage constitutive modeling of rock. Aiming at the problem of the Hoek–Brown (H–B) strength criterion having a large strength prediction value under high confining pressure, the H–B strength criterion is corrected by considering the influence of the initial cracks on the development of the rock strength, and its applicability is verified. Based on the damage theory, assuming that the rock strength microelement obeys the Weibull distribution and considering the influence of residual strength, the damage correction coefficient is introduced, and a thermal damage statistical constitutive model that can reflect the whole process of the development of initial cracks inside the rock is established. The degree of penetration up to the damage is established, and the method of determining the parameters of the model is given. The theoretical curves of the established model are compared and analyzed with the curves of a conventional triaxial compression test of rock samples, and the study shows that the statistical constitutive model of the thermal damage of rock, established based on the modified H–B strength criterion, can better simulate the stress–strain relationship of rock under a conventional triaxial test. It also verifies the reasonableness and applicability of the model, which is expected to provide a basis for the exploitation of deep resources and the safety assessment of underground engineering.



Citation: Lu, T.; Wu, H.; Yin, S.; Xu, X. Study of Rock Damage Constitutive Model Considering Temperature Effect Based on Weibull Distribution. *Appl. Sci.* **2024**, *14*, 3766. <https://doi.org/10.3390/app14093766>

Academic Editor: Tiago Miranda

Received: 12 March 2024

Revised: 22 April 2024

Accepted: 26 April 2024

Published: 28 April 2024

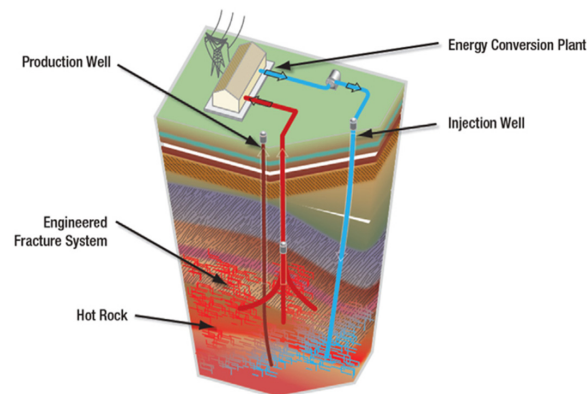


Copyright: © 2024 by the authors. Licensee MDPI, Basel, Switzerland. This article is an open access article distributed under the terms and conditions of the Creative Commons Attribution (CC BY) license (<https://creativecommons.org/licenses/by/4.0/>).

Keywords: rock mechanics; modified strength criterion; Weibull distribution; constitutive model

1. Introduction

With the depletion of surface and shallow resources, mines have entered a state of deep resource mining. However, the high-temperature and high-confining-pressure environment in deep rock mining also brings challenges to the safe construction of underground engineering. For example, the carbonate rock thermal reservoir in the Xiong'an New Area is rich in geothermal resources, and its buried depth is 1000–2000 m underground. The ambient temperature can reach more than 60 °C, and the surrounding geological structure is complicated, making construction and exploitation difficult [1]. For effective exploitation of geothermal resources, EGS (enhanced geothermal systems)-type geothermal power plants are rapidly developing, as shown in Figure 1a [2]. The maximum buried depth of the surrounding rock of the Danba Hydropower Station is 1220 m, the maximum ground stress is more than 30 MPa, which is close to the strength of the surrounding rock in the project, and its soft rock deformation problem is prominent [3]. As shown in Figure 1b [4], the deformation of the Muzhailing Tunnel even reaches 2.3 m. The problems of high temperatures and high confining pressures in these deep rocks put forward higher requirements for the safety and reliability of practical engineering, so it is of great significance to study the strength and deformation of rocks under high temperatures and high confining pressures.



(a) Basic layout of an EGS-type geothermal plant and its purpose for being used.



(b) Large deformation of the local vault in Muzhailing Tunnel.

Figure 1. Examples of underground engineering.

As a macroscopic characterization of the rock strength microelement, the rock strength criterion is the basis for the establishment of the rock constitutive model. A The rock constitutive model is a mathematical model describing the mechanical properties and mechanical behavior of rocks, which is crucial to the understanding of the deformation, the stress response as well as the behavior of the rock structure under different loading conditions. For this reason, scholars have carried out a lot of research on the strength criterion and the constitutive model of rocks. Li et al. [5] corrected the strength criterion error under different confining pressures of rocks and effectively solved the problem of a large strength prediction under high confining pressure by considering the error between the predicted strength and actual strength of the Hoek–Brown (H–B) criterion as a quadratic term with respect to the confining pressure, and they gave a formula for calculating the critical confining pressure. Guo et al. [6] proposed the generalized Drucker–Prager (D–P) strength criterion from the perspective of the releasable strain energy of rocks, which solved the problem of the D–P strength criterion having large stress in the tensile–shear zone and which did not have the stress angle effect.

Guo et al. [7] modified the Mohr–Coulomb (M–C) strength criterion by introducing the principle of elastic strain energy, reflecting the effect of the medium principal stresses in the deformation process of rocks. Hu et al. [8] combined the theory of the criterion of the maximum energy release rate of the rock rupture process with the theory of the maximum energy release rate of the rock rupture process, which gave results related to the thermal damage and initial cracking of the rocks under high-temperature conditions from a microscopic point of view. The parameter value of the H–B strength criterion related to the thermal damage and initial cracking in rocks under high-temperature conditions was given, and the reasonableness of the parameter value was proved with a large amount of data. Pan et al. [9] established a statistical damage constitutive model reflecting the compaction stage and residual strength of rock by considering the compaction stage before the peak of the stress–strain curve and the existence of residual strength. Li et al. [10] used a

bio-retarded growth model to characterize the evolution of the internal crack length of rocks and established an ontological model for the damage evolution of rocks, which exposed the force mechanism of damaged rocks from a microscopic point of view. Zhang et al. [11] established a statistical damage ontology model for rocks by using the generalized formula for the strength criterion of rocks and took into account the change in the strain rate during the stressing process of rocks, which better simulated the damage process of rocks under different confining pressures and different strain rate conditions.

Although the D–P strength criterion considers the effect of intermediate principal stress on strength, it cannot effectively distinguish the difference between the meridional limit lines of tensile and compressive rock. In addition, it is inconsistent with the results of triaxial tests on rocks, so it is rarely applied in rock mechanics [12]. The M–C strength criterion and the H–B strength criterion are the most widely used strength criteria at present. Although the M–C strength criterion is widely used in geotechnical materials, it is unable to consider the brittle–ductile transformation characteristics of geotechnical materials in the process of large interval variations in the confining pressure because it is a linear strength criterion [13]. The H–B strength criterion obtains the relevant strength criterion parameters empirically, which can characterize the brittle–ductile transformation characteristics of rocks under high confining pressures to a certain extent, so the H–B strength criterion is more in line with reality. However, the H–B strength criterion still has some limitations, i.e., strength predictions of the H–B strength criterion for geotechnical materials are still larger under high confining pressures [14,15]. Yu et al. [16] found that the predicted strength values of the H–B strength criterion are still larger than the experimental values due to the compression thawing and crushing of internal cracks in permafrost under high confining pressures.

Considering the expansion and penetration of the initial cracks in the rock during the stressing process, as well as the influence of the initial thermal damage and thermogenic cracks on the strength of the rock at high temperatures [17], the modified H–B strength criterion is introduced. And, based on the statistical damage theory, new damage correction coefficients are adopted to establish a statistical thermal damage constitutive model that can respond to the initial cracks and thermogenic cracks in the rock, with the aim of providing a basis for the extraction of deep resources and the safety assessment of underground engineering.

2. Statistical Thermal Damage Constitutive Modeling of Rocks

2.1. Applicability of the Strength Criterion

The empirical H–B strength criterion proposed by E. Hoek and E. T. Brown [18–22] is

$$\sigma_1 = \sigma_3 + \sigma_u \sqrt{m \frac{\sigma_3}{\sigma_u} + s} \quad (1)$$

$$m = m_i \exp\left(\frac{GSI - 100}{28}\right) \quad (2)$$

where σ_1 and σ_3 are the maximum and minimum principal stress of rock failure, respectively, σ_u is the uniaxial compressive strength of rock and s represents the empirical parameters of the rock. For intact undisturbed rock, $s = 1$. m_i is the reflecting rock hardness, and GSI is the geological strength index where the rock is located. The above formula is converted into

$$(\sigma_1 - \sigma_3)^2 = m\sigma_u\sigma_3 + \sigma_u^2 \quad (3)$$

In order to better characterize rock strength, Hu et al. [7] used Griffith fracture theory to simulate existing microscopic cracks from a fine-grained point of view, combined with the theory of the maximum energy release rate criterion of the rock rupture process, and they found that the strength of the rock samples with bigger initial damage was lower, as shown in Equation (4):

$$\sigma_1 = M(\mu, D_0)\sigma_3 + N(\mu, D_0) \frac{K_{IC}}{\sqrt{\pi c}} \quad (4)$$

where K_{IC} is the type I fracture factor of the rock, c is half the initial length of the crack and $M(\mu, D_0)$ and $N(\mu, D_0)$ are parameters related to the coefficient of friction and initial damage.

The value of parameter m of the H–B strength criterion is related to the initial crack friction coefficient and temperature of the rock, and the following method was proposed to obtain the value of the relevant parameter ψ_T by fitting existing test data and then obtaining the value of parameter m of the strength criterion, as shown in Equation (5):

$$m = \frac{\varphi\psi_T}{k(\sqrt{1+\varphi^2}-\varphi)} \quad (5)$$

where ψ_T is a parameter related to the initial crack density and temperature of the rock, which can be obtained by the fitting method, φ is the coefficient of internal friction of the rock and k is an internal parameter related to the fracture damage criterion of the rock, which is taken as $\sqrt{3}/2$ in the maximum stress criterion and which is taken as 1 in the maximum energy release rate criterion [23].

Substituting Equation (5) into Equation (3) yields

$$(\sigma_1 - \sigma_3)^2 = \frac{\varphi\psi_T}{k(\sqrt{1+\varphi^2}-\varphi)} \sigma_u \sigma_3 + \sigma_u^2 \quad (6)$$

Mining of deep rocks is accompanied by deformation of the rock and collapse of the roadway. For example, the Xincheng gold mine in Jincheng Town, Laizhou City, Shandong Province, China, was mined to a depth of more than 1200 m. Even with appropriate support, the granite of the roadway generally undergoes local deformation, which can destabilize over time and lead to the collapse of the roadway perimeter rock [24]. Therefore, it is of great significance to study the mechanical behavior of granite under high perimeter pressure.

In deep engineering, rock bursts and tunnel deformation problems are prominent, in which the rock explosion problem of marble is prominent. For example, the Jinping hydropower station has experienced rock explosions many times, which have become a typical case in the analysis of related accidents [25]. Huang et al. [26] conducted a series of triaxial creep tests on deep Jinping marble, revealing coupling between excavation damage and high pore pressure. Zhao et al. [27] used true triaxial creep experiments to study the transient deformation, creep rate and long-term strength of Jinping marble under different three-dimensional stress states.

The problem of large deformations in deep tunnels rich in sandstone and limestone is prominent. Zhang et al. [4] investigated large deformations of thin-layer soft rock in the No. 2 inclined shaft of the Muzhailing Tunnel through the discrete element numerical simulation method. The presence of soft rock such as sandstone and limestone is the main reason for large deformations in the tunnel. Rao et al. [28] conducted a deformation study of soft rock based on the gray prediction method, and the control of different support schemes was analyzed by numerical simulation.

Taking into account the engineering problems associated with the above typical rocks, granite [29], limestone [30], marble [31] and sandstone [32] were selected for this study. The corresponding test data and mechanical parameters are shown in Table 1. The friction angle can be obtained by fitting the perimeter pressure to the strength, the internal friction coefficient is the tangent of the internal friction angle, and ψ_T and $m\sigma_u$ are obtained by fitting the experimental data in Table 1.

As shown in Figure 2, the predicted strengths using the modified strength criterion in this paper have a good fit to experimental values of more than 0.95, and the strength criterion that takes into account the presence of initial cracks is more accurate in predicting rock strength compared with the original H–B strength criterion. Although the H–B strength criterion takes into account the effect of confining pressure to a certain extent, the predicted strengths are still higher to a certain extent than the experimental values

under high confining pressures, whereas the modified H–B strength criterion overcomes this shortcoming by taking into account the presence of initial cracks in the parameter acquisition process. The modified H–B strength criterion adopted in this paper solves the problem of the predicted stresses of rocks under high confining pressure being too large, which shows that the modified H–B strength criterion can better evaluate the strength properties of rocks.

Table 1. Mechanical parameters of various rocks under different confining pressures.

Rock Type	Confining Pressure/MPa	Peak Strength/MPa	Internal Friction Angle/ $^{\circ}$	φ	ψ_T	$m\sigma_u$ /MPa	R^2
Granite	0	116.852	47.36	1.08	8.493	2808.47	0.9571
	10	208.038					
	20	301.143					
	30	370.961					
	40	364.571					
Limestone	0	65.525	34.56	0.69	2.687	352.13	0.9738
	2	77.088					
	4	83.512					
	5	85.653					
	8	96.360					
	10	102.784					
	15	112.206					
	20	128.908					
Marble	0	53.115	46.99	1.07	7.842	958.98	0.9962
	5	126.738					
	10	173.766					
	20	245.427					
	30	303.524					
Sandstone	0	55.69	26.39	0.50	3.262	583.06	0.9983
	5	84.57					
	10	107.37					
	15	125.43					
	25	156.80					
	35	186.43					

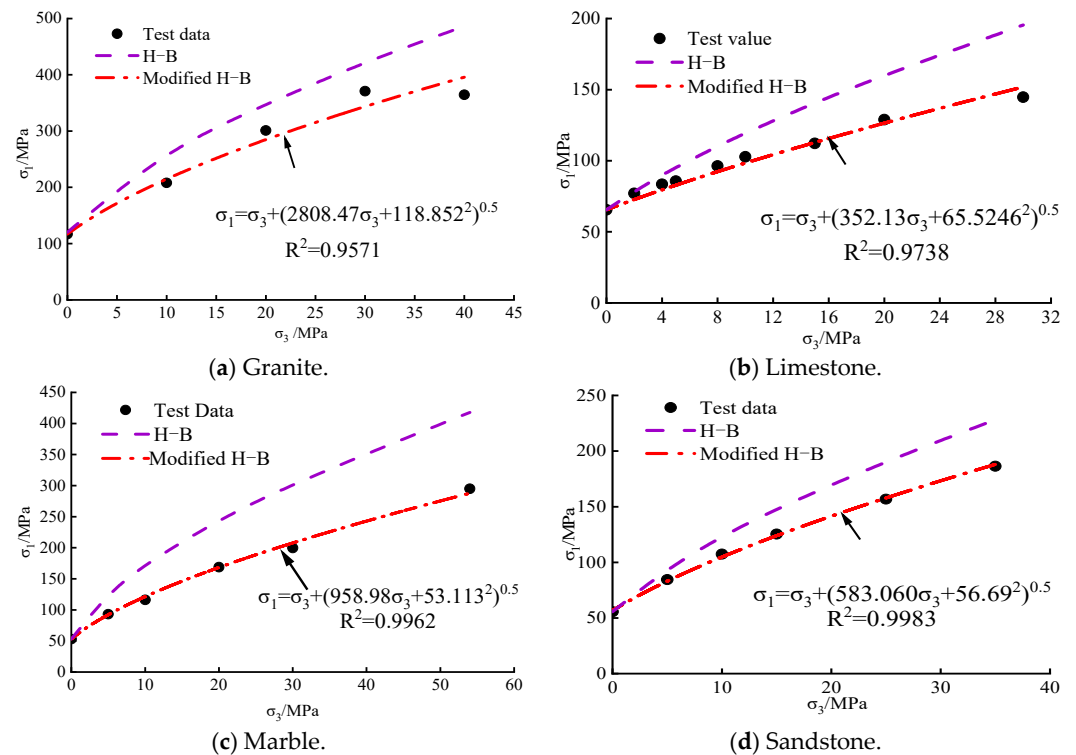


Figure 2. Relationship between strength criterion and test strength.

The strength predictions of the H–B strength criterion and the modified H–B strength criterion under different confining pressures are shown in Figure 2.

2.2. Establishment of a Constitutive Model

In order to better simulate the stress–strain relationship of rock under high confining pressures, a statistical thermal damage constitutive model of rock based on the above modified strength criterion and the statistical damage theory of rock is proposed. Equation (3) is transformed into a stress-invariant representation:

$$\begin{aligned}
 F(I_1^*, J_2^*, \theta_\sigma) &= \frac{\varphi\psi_T}{k(\sqrt{1+\varphi^2}-\varphi)}\sigma_u \frac{I_1^*}{3} + 4J_2^* \cos^2 \theta_\sigma \\
 &+ \frac{\varphi\psi_T}{k(\sqrt{1+\varphi^2}-\varphi)}\sigma_u \sqrt{J_2^*} \left(\cos \theta_\sigma + \frac{\sin \theta_\sigma}{\sqrt{3}} \right) \\
 &= \sigma_u^2
 \end{aligned}
 \tag{7}$$

Here,

$$I_1^* = \sigma_1^* + \sigma_2^* + \sigma_3^* = \frac{(\sigma_1 + \sigma_2 + \sigma_3)E\varepsilon_1}{\sigma_1 - \mu(\sigma_2 + \sigma_3)}
 \tag{8}$$

$$\begin{aligned}
 J_2^* &= \frac{1}{6} \left[(\sigma_1^* - \sigma_2^*)^2 + (\sigma_1^* - \sigma_3^*)^2 + (\sigma_2^* - \sigma_3^*)^2 \right] \\
 &= \frac{E^2\varepsilon_1^2(\sigma_1^2 + \sigma_2^2 + \sigma_3^2 - \sigma_1\sigma_2 - \sigma_2\sigma_3 - \sigma_1\sigma_3)}{3[\sigma_1 - \mu(\sigma_2 + \sigma_3)]^2}
 \end{aligned}
 \tag{9}$$

$$\tan \theta_\sigma = \frac{2\sigma_2 - \sigma_1 - \sigma_3}{\sqrt{3}(\sigma_1 - \sigma_3)}
 \tag{10}$$

The nominal stress values σ_1 , σ_2 and σ_3 and the strain value ε_1 corresponding to the principal stress can be obtained from the conventional triaxial test of the rock, and the result of the corresponding effective stresses are σ_1^* , σ_2^* and σ_3^* . θ_σ is known as the Lode Angle, and E is the elastic modulus of the rock.

In conventional triaxial tests, $\sigma_2 = \sigma_3$ and $\sigma_2^* = \sigma_3^*$, so Equations (8)–(10) can be transformed into

$$I_1^* = \frac{(\sigma_1 + 2\sigma_3)E\varepsilon_1}{\sigma_1 - 2\mu\sigma_3}
 \tag{11}$$

$$J_2^* = \frac{E^2\varepsilon_1^2(\sigma_1 - \sigma_3)^2}{3(\sigma_1 - 2\mu\sigma_3)^2}
 \tag{12}$$

$$\theta_\sigma = 30^\circ
 \tag{13}$$

By substituting Equations (11)–(13) into Equation (7),

$$f(\sigma) = \sigma_u^2 = \frac{\varphi\psi_T}{k(\sqrt{1+\varphi^2}-\varphi)}\frac{\sigma_u\sigma_1E\varepsilon_1}{\sigma_1 - 2\mu\sigma_3} + \left(\frac{(\sigma_1 - \sigma_3)^2E^2\varepsilon_1^2}{\sigma_1 - 2\mu\sigma_3} \right)^2
 \tag{14}$$

In this paper, the mechanical damage variable D_M is defined as the ratio of damaged elements (N_{dam}) to the total number of elements (N_{tol}) of rock material under a load:

$$D_M = \frac{N_{dam}}{N_{tol}}
 \tag{15}$$

Suppose that the strength of rock elements follows the Weibull distribution:

$$N_{dam} = \int_0^f N_{tol} \frac{n}{F} \left(\frac{f}{F} \right)^{n-1} \exp \left[- \left(\frac{f}{F} \right)^n \right] df
 \tag{16}$$

where n and F are the distribution parameters subject to the Weibull distribution, and the mechanical damage value under a normal temperature can be obtained by connecting Equations (15) and (16):

$$D_M = \int_0^{f(\sigma)} P(f)df = 1 - \exp\left[-\left(\frac{f(\sigma)}{F}\right)^n\right] \tag{17}$$

The thermal damage value of rocks at high temperatures D_T is defined as

$$D_T = 1 - \frac{E_T}{E_0} \tag{18}$$

E_T is the elastic modulus at high temperatures, and E_0 is the rock elastic modulus at room temperature.

Considering the coupling of the thermal damage and mechanical damage of the rocks under high temperature conditions, the total damage value of the rocks is defined as [33]

$$D = D_M + D_T - D_M D_T \tag{19}$$

Considering that the initial thermal damage value of rock at normal temperatures is 0, the damage value of rock at normal temperatures is therefore considered $D = D_M$.

Considering the influence of rock residual strength, the rock damage correction coefficient δ is introduced, which is defined as

$$\delta = \sqrt{\frac{\sigma_p - \sigma_r}{\sigma_p}} \tag{20}$$

where σ_p is the peak strength of the rock and σ_r is the residual strength of the rock.

According to the rock strain equivalence hypothesis [34],

$$\sigma_i^* = \frac{\sigma_i}{1 - \delta D}, (i = 1, 2, 3) \tag{21}$$

Assuming that rocks obey a generalized view of Hooke’s law before failure,

$$\varepsilon_i = \frac{1}{E} [\sigma_i^* - \mu(\sigma_j^* + \sigma_k^*)], (i, j, k = 1, 2, 3) \tag{22}$$

Combining Equations (21) and (22), we obtain

$$\varepsilon_i = \frac{1}{E(1 - \delta D)} [\sigma_i - \mu(\sigma_j + \sigma_k)], (i, j, k = 1, 2, 3) \tag{23}$$

In conventional triaxial tests, the above formula is converted to

$$\sigma_1 = E\varepsilon_1(1 - \delta D) + 2\mu\sigma_3 \tag{24}$$

By combining (17)–(19) and (24), the statistical constitutive model of thermal damage to rock can be obtained as

$$\sigma_1 = E\varepsilon_1 \left\{ 1 - \delta D_T + (D_T - \delta) \left\{ 1 - \exp\left[-\left(\frac{\varphi\psi_T}{k(\sqrt{1 + \varphi^2} - \varphi)} \frac{\sigma_u\sigma_1 E\varepsilon_1}{F\sigma_1} + \frac{\sigma_1^2 E^2 \varepsilon_1^2}{F\sigma_1^2}\right)^n\right]\right\} \right\} + 2\mu\sigma_3 \tag{25}$$

3. Determination of Model Parameters

In order to determine the values of the distribution parameters n and F of the model, this paper adopts the peak point method [13] to arrive at a solution.

From the extreme value characteristics of the stress–strain curve,

$$\sigma \Big|_{\varepsilon=\varepsilon_p} = \sigma_p \tag{26}$$

$$\frac{\partial \sigma}{\partial \varepsilon} \Big|_{\varepsilon=\varepsilon_p} = 0 \tag{27}$$

The expression of parameter n obtained by coupling (25)–(27) is as follows:

$$n = \frac{F \Big|_{\sigma_1=\sigma_p, \varepsilon_1=\varepsilon_p}}{\varepsilon_p \frac{dF}{d\varepsilon_1} \Big|_{\sigma_1=\sigma_p, \varepsilon_1=\varepsilon_p} \ln \left(\frac{(\delta - D_T)E\varepsilon_p}{\sigma_p - 2\mu\sigma_3 + (\delta - 1)E\varepsilon_p} \right)} \tag{28}$$

At the peak point of the stress–strain curve $F \Big|_{\sigma_1=\sigma_p, \varepsilon_1=\varepsilon_p} = \varepsilon_p \frac{dF}{d\varepsilon_1} \Big|_{\sigma_1=\sigma_p, \varepsilon_1=\varepsilon_p}$, the above formula can be simplified as

$$n = \frac{1}{\ln \left[E\varepsilon_p \delta (1 - D_T) / (\sigma_p - 2\mu\sigma_3 + (\delta - 1)E\varepsilon_p) \right]} \tag{29}$$

The relationship between parameter F and parameter n can be expressed as

$$F = \sqrt[n]{n} f(\sigma) \Big|_{\sigma_1=\sigma_p, \varepsilon_1=\varepsilon_p} \tag{30}$$

4. Model Validation and Parameter Analysis at Room Temperature

4.1. Model Validation

A selection of the data of granite at normal temperatures in the literature [29] is made in order to verify the statistical thermal damage constitutive model established in this paper. The mechanical parameters of granite at normal temperatures are shown in Table 2.

Table 2. Mechanical parameters of granite under different confining pressures.

Confining Pressure /MPa	Peak Strength /MPa	Peak Strain /10 ⁻³	Residual Strength /MPa	Residual Strain /10 ⁻³	δ	λ
0	116.852	4.147	7.082	7.037	0.940	0.865
10	208.038	6.805	17.210	8.200	0.958	0.910
20	301.143	7.557	108.000	10.096	0.801	0.877
30	370.961	9.458	107.714	14.111	0.842	0.867
40	364.571	11.394	144.000	18.546	0.704	0.646

The samples were taken from the granite of a mine in Weifang, Shandong Province, and were processed into standard cylindrical samples with a diameter of 50 mm and a length of 100 mm according to the standards of the International Society for Rock Mechanics (ISRM), with an error of ±0.5 mm. The average density of the samples at room temperature was 2.612 g/cm³, and the uniaxial compressive strength was 116.852 Mpa. Among them, feldspars were mainly sodium feldspars, and mica was mainly acicular mica.

During testing, the samples were heated to 25 °C, 200 °C, 400 °C, 600 °C, and 800 °C. In order to ensure uniformity of the heat inside the rock samples, each piece of rock sample was kept at a constant temperature for 2 h after heating, and then the furnace was opened and naturally cooled to room temperature, with 5 pieces of sample at each temperature point, making a total of 25 pieces of rock samples. Then, the MTS815.02 electro-hydraulic servo material testing system from the State Key Laboratory of Deep Geotechnics and Underground Engineering of China University of Mining and Technology was used to conduct conventional triaxial compression tests on the heated rock samples, with the peripheral pressure set to five levels: 0, 10, 20, 30 and 40 Mpa. During the test, a predetermined peripheral pressure was first applied to the rock samples to keep the samples

in hydrostatic pressure, and then the samples were loaded axially at a displacement rate of 0.003 mm/s until the samples were damaged. The peak strength of the samples was reached, and then the MTS815.02 electro-hydraulic servo material testing system continued to apply pressure to the samples and recorded the post-peak stress and deformation of the samples so as to obtain the full stress–strain curves of the samples under triaxial compression. After reaching the peak strength, the MTS815.02 hydraulic servo material testing system continued to apply pressure to the sample and recorded the post-peak stress and deformation of the sample so as to obtain the full stress–strain curves of the samples under triaxial compression.

The parameter values under different confining pressures in Table 1 were substituted into the model established in this paper, and the obtained model curve is shown in Figure 3.

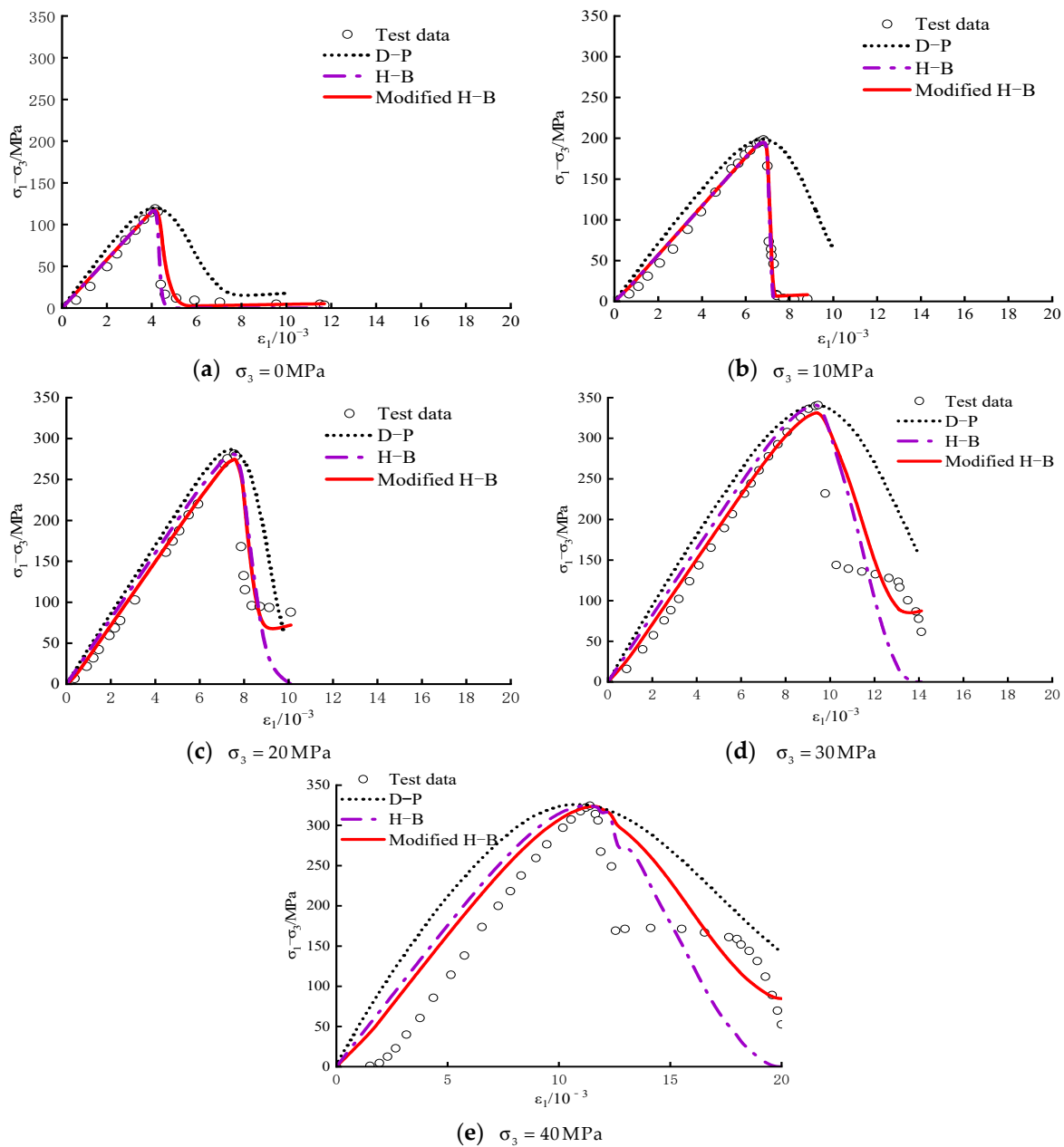


Figure 3. Theoretical and experimental curves under different confining pressures.

Under low confining pressures (0–10 MPa), the model that was established based on the revised strength criterion can better characterize the pre-peak stress–strain relationship

of rock in the pre-peak stage compared to the model established based on the original strength criterion, and the constitutive model established based on the modified H–B strength criterion can better characterize the stress drop and residual strength in the post-peak stage due to the consideration of the damage repair value. With the increase in confining pressure, the brittleness of the rock decreases, and the rock changes from brittle failure to ductile failure. Under high confining pressures (20–40 Mpa), the two models began to distinguish before the peak, and the model based on the modified strength criterion was better than the original strength criterion, in agreement with the test curve.

To further validate the selection of rock samples for model reliability, a reliability analysis of the model was performed by quoting the reliability indices from ref. [30]:

$$\lambda = 1 - \frac{1}{m} \sum_{i=1}^m \left(\frac{|\sigma_{(i)} - \sigma_i|}{\sigma_i} \right) \tag{31}$$

where $\sigma_{(i)}$ is the predicted principal stress value of the rock, σ_i is the principal stress value of the rock test sample and n is the number of samples to verify reliability. The calculation results are shown in Table 2.

From Table 2, it can be seen that the correlation coefficients between each model curve and the experimental curves at room temperature are above 0.85 except at the high confining pressure of 40 Mpa, which proves its good applicability.

Compared with the model that was established based on the modified strength criterion and the D–P criterion [35], the fitting degree of the model established based on the revised H–B strength criterion is superior to the former under various confining pressure conditions, which further indicates the reasonableness of the model.

The value of the rock residual strength is related to the value of the rock correction coefficient δ . In order to further predict rock residual strength, the correction coefficient was introduced, as shown in Equation (20). The calculation method [36] and Equation (20) with the existing correction coefficient were substituted into the model in this paper, and the residual strength value was obtained as shown in Figure 4. The correction coefficient in Equation (20) was obviously more reasonable.

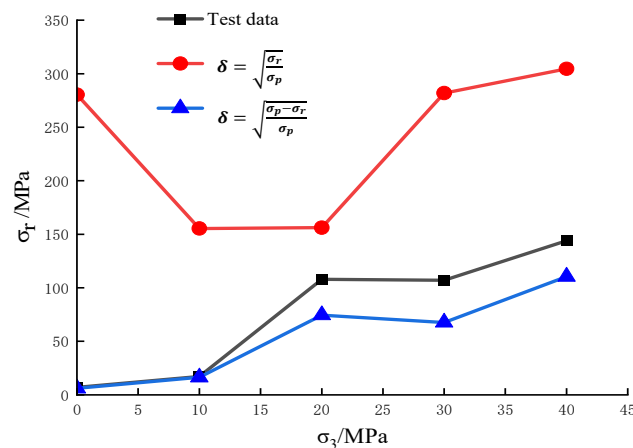


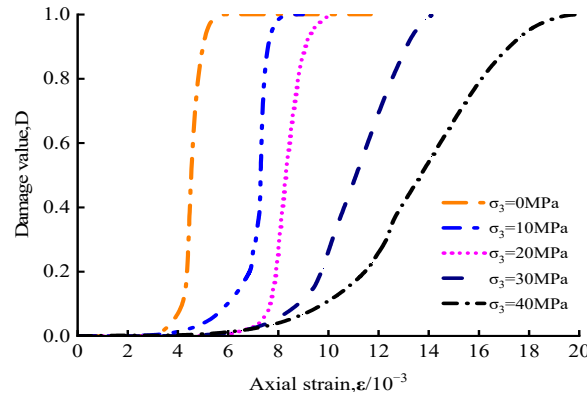
Figure 4. Relationship between residual strength and confining pressure of granite.

As shown in Figure 5a, the relationship between the rock damage value and strain value under different confining pressures is drawn.

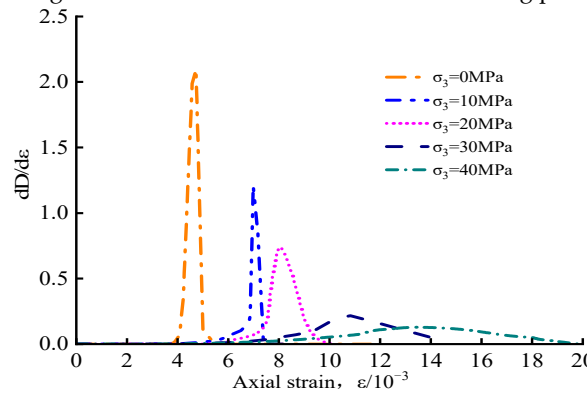
At the same time, based on Figure 5a, the damage evolution curve was differentiated to obtain the damage evolution rate curve of the rock, as shown in Figure 5b.

Taking into consideration the fact that the initial thermal damage of rocks at room temperature (25 °C) is 0 and that the damage evolution curves of rocks under different confining pressures all show an “S” shape, the rock damage evolution curve can be divided into three stages. In the first stage, the initial cracks are gradually closed, the rock samples

are in a stage of compaction and linear elasticity, and the damage evolution curve remains horizontal. In the second stage, with the increase in stress, the initial crack is completely closed, new cracks begin to appear inside the rock, and the cracks gradually expand and penetrate. This results in macroscopic cracks, and the damage value gradually increases until the rock is completely broken. In the third stage, the damage value does not increase after the rock is completely broken, and the damage value reaches 1.



(a) Damage evolution curves under different confining pressures.



(b) Damage evolution rate curves under different confining pressures.

Figure 5. Damage evolution of granite under different confining pressures.

The relationship between the maximum damage evolution rate of rocks and confining pressure is further studied, as shown in Figure 6. The maximum damage evolution rate of rocks decreases exponentially, and the fitting curve and correlation coefficient are as follows:

$$y = 2.451 e^{(-\frac{x}{23.433})} - 0.358, R^2 = 0.982 \tag{32}$$

where x represents the confining pressure value of the rock and y represents the maximum damage evolution rate value of the rock.

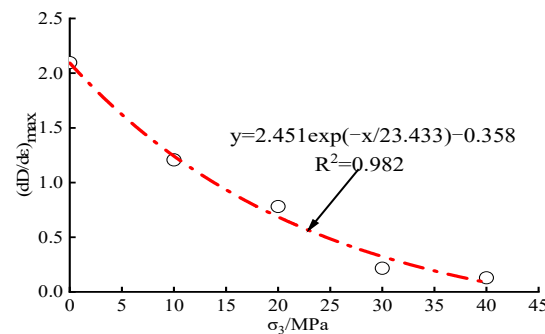


Figure 6. Relationship between distribution parameters and confining pressures.

4.2. Model Parameter Analysis

In order to investigate the physical significance of distribution parameters n and F of the model, the distribution parameter values under each confining pressure can be obtained by calculating Equations (29) and (30). Some scholars have studied the influence of n and F on rock stress–strain curves [37–39], but few studies have been made on the relationship between n and F and confining pressure. The variation in the distribution parameters with the confining pressure is shown in Figure 7.

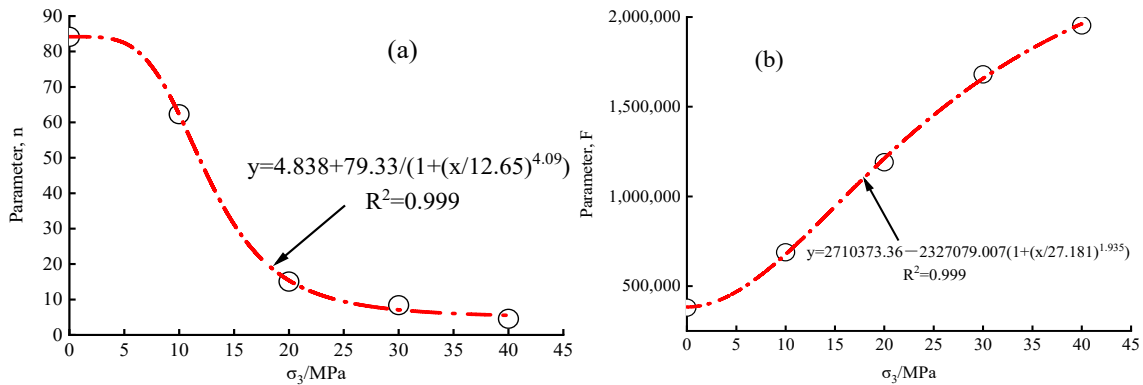


Figure 7. Relationship between distribution parameters and confining pressure.

It can be seen that parameter n gradually decreases with the increase in confining pressure in the form of a logistic function, whereas parameter F gradually increases with the increase in the confining pressure in the form of a logistic function.

$$y = 4.838 + \frac{79.33}{\left[1 + \left(\frac{x}{12.65}\right)^{4.09}\right]}, R^2 = 0.999 \tag{33}$$

where x represents the confining pressure value during the rock test and y represents the value of Weibull distribution parameter n .

$$y = 2710373.36 - \frac{2327079.007}{\left[1 + \left(\frac{x}{27.181}\right)^{1.935}\right]}, R^2 = 0.999 \tag{34}$$

where x represents the confining pressure value during the rock test and y represents the value of Weibull distribution parameter F .

The increase in the confining pressure leads to the transformation of the rock from brittle failure to ductile failure. Therefore, parameter n can characterize the degree of the brittle failure of rock, and parameter F can be used to characterize the macroscopic strength of rock as the change trend and peak strength of the rock increase with the increase in the confining pressure [40–43]. With the increase in the confining pressure, the degree of the brittle failure of the rock decreases gradually, and the value of the strength of the rock increases.

5. The Damage Constitutive Model under a Thermo-Mechanical Coupling Condition Is Considered

The strength value of the rock is further reduced after high-temperature treatment, and the thermal damage value of the rock is related to the thermal crack from a microscopic point of view. In order to further consider the thermal damage value of rocks under high-temperature conditions, the same method as described above was used to obtain the values of the H–B strength criterion parameters at high temperatures. Test data [29] of granite under high-temperature conditions were selected, as shown in Table 3.

Table 3. Rock peak strength and confining pressure at different temperatures.

Temperature/°C	Confining Pressure/MPa	Peak Strength/MPa
200	0	118.800
	10	197.785
	20	276.863
	30	427.773
	40	450.177
400	0	98.548
	10	231.120
	20	335.685
	30	376.763
	40	449.585
600	0	55.974
	10	191.372
	20	312.832
	30	364.602
	40	420.354
800	0	41.706
	10	139.573
	20	272.275
	30	292.180
	40	360.190

The relationship between the modified H–B strength criterion values and the test values at different confining pressures can be obtained, as shown in Figure 8.

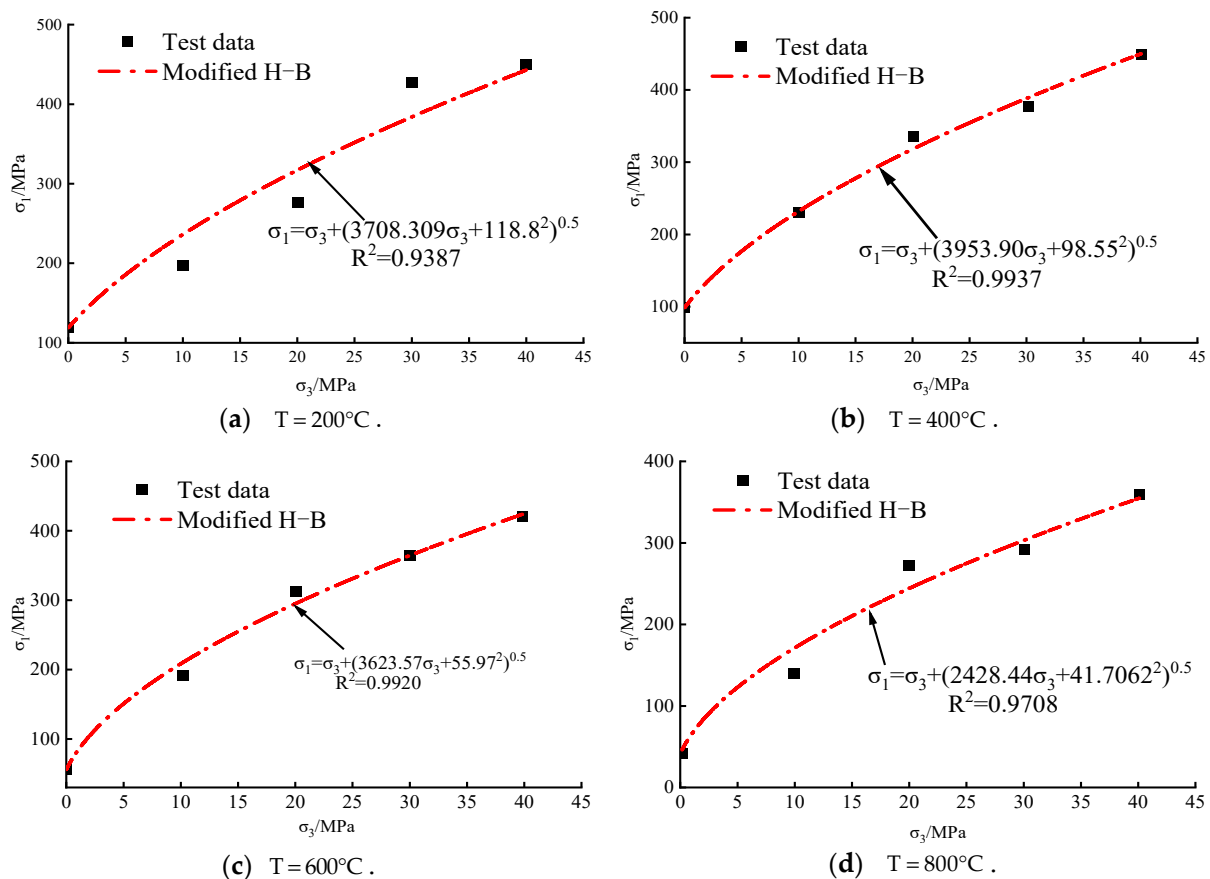


Figure 8. Fitting curves for the modified H–B strength criterion at different temperatures.

In order to further investigate the applicability of the intrinsic model based on the modified H–B strength criterion under high peripheral pressure, the uniaxial test data of granite at high temperatures were selected for verification, and the data obtained from the uniaxial test of granite are shown in Table 4.

Table 4. Mechanical parameters of granite after high-temperature treatment.

Temperature/°C	Peak Strength/MPa	Residual Strength/MPa	δ	Thermal Damage Value	λ
200	118.800	7.412	0.968	0.086	0.820
400	98.529	11.76	0.938	0.120	0.676
600	54.070	1.744	0.984	0.656	0.751
800	41.132	7.724	0.901	0.724	0.786

As shown in Figure 9, under high-temperature conditions, the model established in this paper is still in good agreement with the test curve. The reliability indices obtained based on Equation (31) are all above 0.65. The predicted residual strength value is also more accurate.

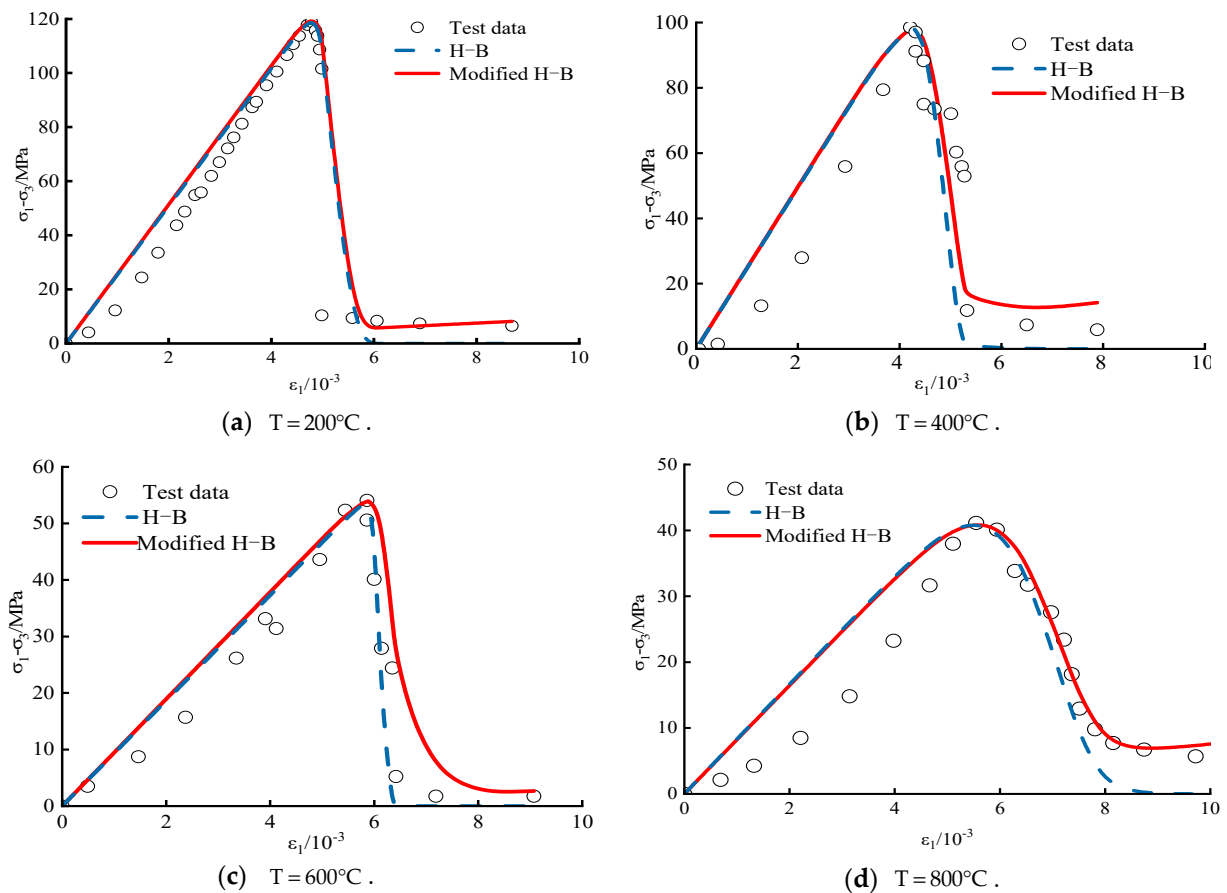


Figure 9. Stress–strain curve of granite at high temperature.

In order to consider the change law of parameters n and F at high temperatures, the relationship curve between temperature and parameters n and F is drawn. As shown in Figure 10, parameter n decreases exponentially with the increase in temperature, and parameter F increases first and then decreases with the increase in temperature. The decrease in parameter n reflects that the brittleness change trend of rock under the condition of increasing temperature is the same as that under the condition of increasing confining pressure. The brittleness drop degree of rock gradually decreases and transforms to ductility.

However, parameter F generally shows a decreasing trend, and the macro strength value of the reaction rock gradually decreases. The reason is that, under high-temperature conditions, the thermal motion of rock molecules is intensified, and the thermal expansion coefficients of various mineral particles composed of granite are different, resulting in a large number of thermal cracks. With the increase in temperature, these thermal cracks gradually spread through the interior of the rock, the deterioration degree of the rock gradually increases, and the peak strength value decreases [44–46].

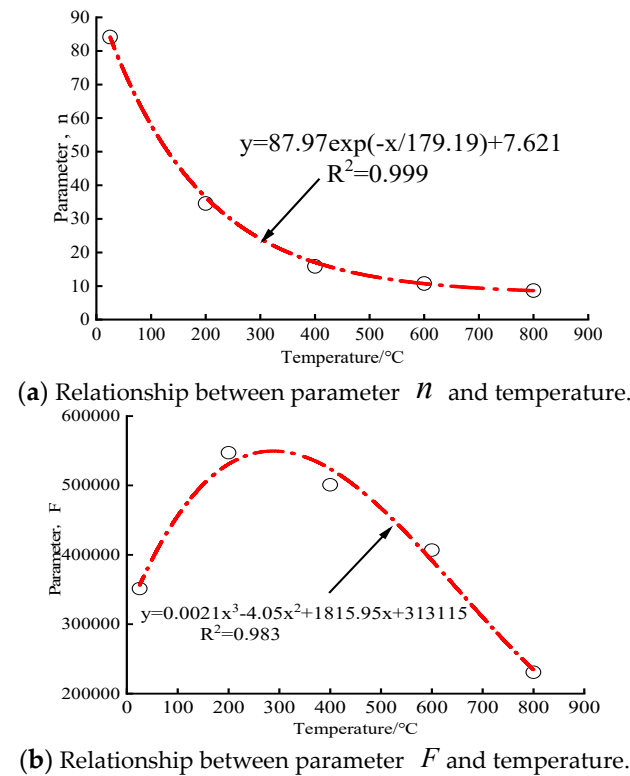


Figure 10. Relationship between distribution parameters and temperature.

The initial thermal damage value of the rock is coupled with the mechanical damage [47,48]. The thermal damage evolution curve obtained after coupling is shown in Figure 11a, and the maximum damage evolution rate of the rock is shown in Figure 11b. Overall, it can be stated that the maximum damage evolution rate of the rock decreases with the increase in temperature.

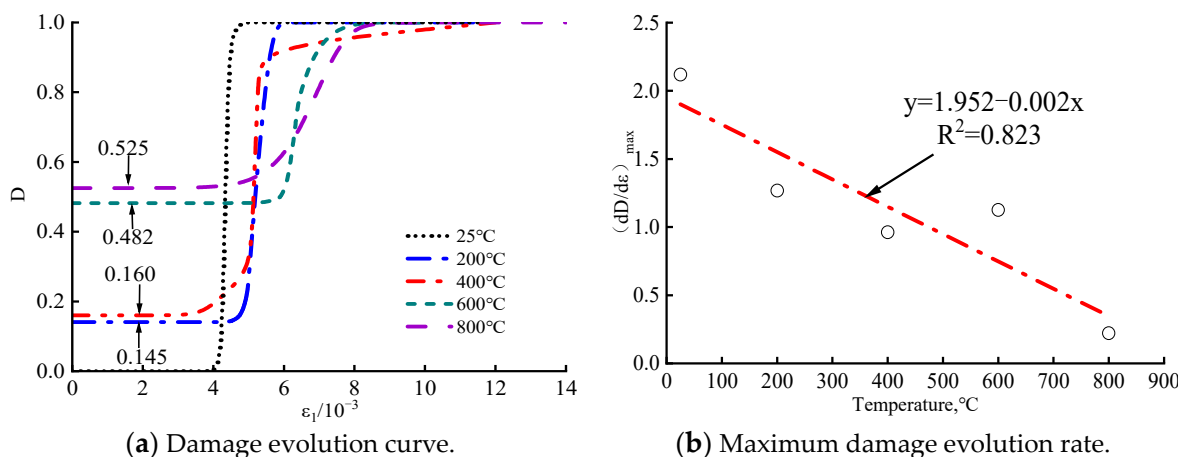


Figure 11. Damage evolution of granite at different temperatures.

6. Conclusion and Discussion

Considering the problem of the high prediction value of the H–B strength criterion for rock strength, the parameter value method of the H–B strength criterion is introduced to consider the crack-related element in the rock failure process, and a new damage correction coefficient is introduced to characterize the residual strength of rock in order to accurately predict the residual strength of rock. A constitutive model of rock statistical thermal damage considering initial crack and temperature correlation is established, and the following conclusions and discussion are drawn:

- (1) Considering the effect of the presence of initial cracks in the rock on the strength of the rock, the H–B strength criterion is modified to solve the problem of the predicted strength value of H–B still being high under high confining pressures. The rationality of the revised strength criterion is verified by selecting rock sample data at normal temperatures and at high temperatures.
- (2) Based on the statistical damage theory, it is assumed that rock strength follows the Weibull distribution, combined with the revised H–B strength criterion and considering the damage correction coefficient related to residual strength. A statistical thermal damage constitutive model of rock under the condition of high temperatures and high confining pressures is established, and the physical significance of the model distribution parameters and their patterns of change, as well as the damage evolution of the rocks, are analyzed. By comparing the model in this paper with the model established by the H–B criterion, the model established in this paper is more consistent with the experimental data and has good applicability, which can provide a reference for the establishment of rock constitutive models under high temperatures and confining pressures.
- (3) The damage correction coefficient selected in this paper can better characterize the residual strength values of rocks and provide reference for the prediction of residual strength values of rocks, but there is still an error between the damage modification coefficients and the actual residual strength values, which needs to be further discussed and improved. In addition, this article only focuses on the investigation of the intrinsic model of the rock under high temperatures and high confining pressures, and the modeling of deep rock under high hydrostatic pressures and high perturbation conditions needs to be further considered in the future.

Author Contributions: Conceptualization, X.X.; methodology, X.X. and T.L.; validation, H.W. and T.L.; formal analysis, S.Y.; investigation, X.X. and T.L.; resources, S.Y. and H.W.; data curation, T.L. and H.W.; writing—original draft preparation, S.Y. and T.L.; writing—review and editing, X.X. All authors have read and agreed to the published version of the manuscript.

Funding: This research was funded by the Open Research Fund of the Key Laboratory of Safety and High-efficiency Coal Mining, Ministry of Education (Anhui University of Science and Technology), No. JYBSYS2020208, and the Innovation Training Program for Jiangsu College Students, No. 202310304153Y. Postgraduate Research & Practice Innovation Program of School of Transportation and Civil Engineering, Nantong University (No. NTUJTXYG12305).

Institutional Review Board Statement: Not applicable.

Informed Consent Statement: Not applicable.

Data Availability Statement: Data are contained within the article.

Conflicts of Interest: The authors declare no conflicts of interest.

References

1. Wang, Y.J.; Liang, W.; Du, Z.Q.; Wang, L.; Zhang, T.; Tong, Z. Exploration of the application of drill bits in the formation of flint dolomite in the D05 well of Xiong'an New Area. *Drill. Eng.* **2023**, *50*, 142–148.
2. Olasolo, P.; Juárez, M.; Morales, M.; D'amico, S.; Liarte, I. Enhanced geothermal systems (EGS): A review. *Renew. Sustain. Energy Rev.* **2016**, *56*, 133–144. [[CrossRef](#)]

3. Wu, A.Q.; Zhu, J.B. Summary of research on mechanical properties and in-situ stress testing of deep rock engineering. *J. Yangtze River Sci. Res. Inst.* **2014**, *31*, 43–50.
4. Zhang, X.; He, M.; Wang, F.; Li, G.; Xu, S.; Tao, Z. Study on the large deformation characteristics and disaster mechanism of a thin-layer soft-rock tunnel. *Adv. Civ. Eng.* **2020**, *2020*, 8826337. [[CrossRef](#)]
5. Li, B.; Xu, M.G.; Liu, Y.Z.; Wang, P. Improvement of Hoek Brown strength criterion for intact rocks under triaxial conditions. *J. Min. Saf. Eng.* **2015**, *32*, 1010–1016.
6. Guo, J.Q.; Jiang, J.G.; Liu, X.R.; Chen, J.X.; Lu, X.F.; Yang, Q.T. Correction of D-P strength criterion based on elastic strain energy. *China Civ. Eng. J.* **2021**, *54*, 110–116.
7. Guo, J.; Liu, X.R.; Huang, W.F.; Luo, X.; Niu, L. Discussion of Mohr-Coulomb strength criterion based on elastic strain energy. *J. Tongji Univ. Nat. Sci. Ed.* **2018**, *46*, 1168–1174. [[CrossRef](#)]
8. Hu, X.; Qi, Y.; Hu, H.; Lei, G.; Xie, N.; Gong, X. A micromechanical-based failure criterion for rocks after high-temperature treatment. *Eng. Fract. Mech.* **2023**, *284*, 109275. [[CrossRef](#)]
9. Pan, Y.W.; Huang, D.W. Statistical damage constitutive model for rocks considering compaction processes and residual strength. *Min. Technol.* **2021**, *21*, 38–42. [[CrossRef](#)]
10. Li, S.N.; Xiao, J.; Li, Y.; Liu, X.; Liang, Q.; Chang, J.; Liu, J. Research on rock damage constitutive model based on microscopic crack propagation evolution. *Chin. J. Rock Mech. Eng.* **2023**, *42*, 640–648. [[CrossRef](#)]
11. Zhang, C.; Yang, C.Q.; Zhu, D.P.; Yang, Z.W.; Xia, Z.R. Applicability analysis of rock deformation statistical damage simulation considering strain rate changes. *Chin. J. Appl. Mech.* **2023**, *40*, 1–10.
12. Ding, S.M.; Zhao, Z.H.; Wang, N.N. Classification and review of rock strength theory. *Water Resour. Archit. Eng.* **2017**, *15*, 95–102. [[CrossRef](#)]
13. Zhang, C.; Yu, J.; Bai, Y.; Cao, W.G.; Zhang, S.; Guo, Z.G. A Statistical damage constitutive model for rock embrittlement transformation based on strength theory. *Chin. J. Rock Mech. Eng.* **2023**, *42*, 307–310.
14. Wang, Z.; Qi, C.; Ban, L.; Yu, H.; Wang, H.; Fu, Z. Modified Hoek–Brown failure criterion for anisotropic intact rock under high confining pressures. *Bull. Eng. Geol. Environ.* **2022**, *81*, 333. [[CrossRef](#)]
15. Ismael, M.; Konietzky, H. Constitutive model for inherent anisotropic rocks: Ubiquitous joint model based on the Hoek-Brown failure criterion. *Comput. Geotech.* **2019**, *105*, 99–109. [[CrossRef](#)]
16. Yang, Y.; Gao, F.; Lai, Y. Modified Hoek-Brown criterion for nonlinear strength of frozen soil. *Cold Reg. Sci. Technol.* **2013**, *86*, 98–103. [[CrossRef](#)]
17. Griffiths, L.; Heap, M.; Baud, P.; Schmittbuhl, J. Quantification of microcrack characteristics and implications for stiffness and strength of granite. *Int. J. Rock Mech. Min. Sci.* **2017**, *100*, 138–150. [[CrossRef](#)]
18. Brown, E.T.; Hoek, E. *Underground Excavations in Rock*; CRC Press: Boca Raton, FL, USA, 1980.
19. Hoek, E.; Kaiser, P.K.; Bawden, W.F. *Support of Underground Excavations in Hard Rock AA BALKEMA*; Rotterdam/Brookfield: Rotterdam, The Netherlands, 1995.
20. Hoek, E.; Kaiser, P.K.; Bawden, W.F. *Support of Underground Excavations in Hard Rock*; CRC Press: Boca Raton, FL, USA, 2000.
21. Hoek, E.; Carranza, T.C.; Corkum, B. Hoek-Brown failure criterion-2002 edition. *Proc. NARMS-Tac* **2002**, *1*, 267–273.
22. Hoek, E.; Brown, E.T. The Hoek–Brown failure criterion and GSI—2018 edition. *J. Rock Mech. Geotech. Eng.* **2019**, *11*, 445–463. [[CrossRef](#)]
23. Nuismer, R.J. An energy release rate criterion for mixed mode fracture. *Int. J. Fract.* **1975**, *11*, 245–250. [[CrossRef](#)]
24. Sun, C.; Jin, C.; Wang, L.; Ao, Y.; Zhang, J. Creep damage characteristics and local fracture time effects of deep granite. *Bull. Eng. Geol. Environ.* **2022**, *81*, 79. [[CrossRef](#)]
25. Zhang, C.Q.; Feng, X.-T.; Zhou, H.; Qiu, S.L.; Wu, W.P. Case histories of four extremely intense rockbursts in deep tunnels. *Rock Mech. Rock Eng.* **2012**, *45*, 275–288. [[CrossRef](#)]
26. Huang, X. Time-Dependent behavior of Jinping deep marble taking into account the coupling between excavation damage and high pore pressure. *Rock Mech. Rock Eng.* **2022**, *2022*, 4893–4912. [[CrossRef](#)]
27. Zhao, J.; Feng, X.T.; Zhang, X.; Yang, C.; Zhou, Y. Time-dependent behavior and modeling of Jinping marble under true triaxial compression. *Int. J. Rock Mech. Min. Sci.* **2018**, *110*, 218–230. [[CrossRef](#)]
28. Rao, J.; Tao, Y.; Xiong, P.; Nie, C.; Peng, H.; Xue, Y.; Xi, Z. Research on the large deformation prediction model and supporting measures of soft rock tunnel. *Adv. Civ. Eng.* **2020**, *2020*, 6630546. [[CrossRef](#)]
29. Xu, X.L.; Gao, F.; Zhang, Z.Z. The effect of confining pressure after high temperature on the deformation and strength characteristics of granite. *Chin. J. Geotech. Eng.* **2014**, *36*, 2246–2252. [[CrossRef](#)]
30. Chen, Y.; Lin, H.; Wang, Y.; Xie, S.; Zhao, Y.; Yong, W. Statistical damage constitutive model based on the Hoek–Brown criterion. *Arch. Civ. Mech. Eng.* **2021**, *21*, 117. [[CrossRef](#)]
31. Walton, G.; Hedayat, A.; Kim, E.; Labrie, D. Post-yield strength and dilatancy evolution across the brittle–ductile transition in indiana limestone. *Rock Mech. Rock Eng.* **2017**, *50*, 1691–1710. [[CrossRef](#)]
32. Xu, S.L.; Wu, W.; Wang, G.Y.; Zhang, Q.H.; Xu, J.P. Study on the whole process of triaxial compression of marble with equal perimeter pressure I: Experiments on the whole process of triaxial compression and the whole process of unloading of perimeter pressure before and after peaks. *Chin. J. Rock Mech. Eng.* **2001**, *20*, 763–767.
33. Zhang, H.M.; Yang, G.S. Research on damage model of rock under coupling action of freeze-thaw and load. *China J. Rock Mech. Eng.* **2010**, *29*, 471–476.

34. Ju, Y.; Xie, H.P. The applicable conditions for defining damage based on the strain equivalence hypothesis. *Chin. J. Appl. Mech.* **1998**, *45–51*, 144–145.
35. Xu, Y.H. *Research on Statistical Damage Constitutive Model of Rock under Thermodynamic Coupling Effect*; Nantong University: Nantong, China, 2016.
36. Cao, R.L.; He, S.H.; Wei, J.; Wang, F. Research on statistical constitutive model of rock damage softening based on residual strength correction. *Rock Soil Mech.* **2013**, *34*, 1652–1660. [[CrossRef](#)]
37. Yu, T. Statistical damage constitutive model of quasi-brittle materials. *J. Aerosp. Eng.* **2009**, *22*, 95–100. [[CrossRef](#)]
38. Ting, C.L.; Lian, X.L.; Shi, L.Z.; Jie, C.S. Development and application of a statistical constitutive model of damaged rock affected by the load-bearing capacity of damaged elements. *J. Zhejiang Univ. SCI. A* **2015**, *16*, 644–655. [[CrossRef](#)]
39. Wang, J.; Song, Z.; Zhao, B.; Liu, X.; Liu, J.; Lai, J. A study on the mechanical behavior and statistical damage constitutive model of sandstone. *Arab. J. Sci. Eng.* **2018**, *43*, 5179–5192. [[CrossRef](#)]
40. Chen, J.T.; Feng, X.T. Constitutive model of hard rock under high ground stress. *Rock Soil Mech.* **2007**, *2007*, 2271–2278.
41. Zhang, C.; Cao, W.G.; Zhao, H.; He, M. Statistical damage simulation method for rock stress-strain curves considering confining pressure effects and brittle strength drop. *Chin. J. Geotech. Eng.* **2022**, *44*, 936–944. [[CrossRef](#)]
42. Chen, Y.; Zhang, L.; Xie, H.; Liu, J.; Liu, H.; Yang, B. Damage ratio based on statistical damage constitutive model for rock. *Math. Probl. Eng.* **2019**, *2019*, 3065414. [[CrossRef](#)]
43. Chen, S.; Qiao, C.; Ye, Q.; Khan, M.U. Comparative study on three-dimensional statistical damage constitutive modified model of rock based on power function and Weibull distribution. *Environ. Earth Sci.* **2018**, *77*, 108. [[CrossRef](#)]
44. Zhou, S.-W.; Xia, C.C.; Zhao, H.-B.; Mei, S.-H.; Zhou, Y. Statistical damage constitutive model for rocks subjected to cyclic stress and cyclic temperature. *Acta Geophys.* **2017**, *65*, 893–906. [[CrossRef](#)]
45. Liu, W.; Dan, Z.; Jia, Y.; Zhu, X. On the statistical damage constitutive model and damage evolution of hard rock at high-temperature. *Geotech. Geol. Eng.* **2020**, *38*, 4307–4318. [[CrossRef](#)]
46. Chen, Z.; Sha, S.; Xu, L.; Quan, J.; Rong, G.; Jiang, M. Damage Evaluation and statistic constitutive model of high-temperature granites subjected to liquid nitrogen cold shock. *Rock Mech. Rock Eng.* **2022**, *55*, 2299–2321. [[CrossRef](#)]
47. Luo, J.; He, J. Constitutive model and fracture failure of sandstone damage under high temperature–cyclic stress. *Materials.* **2022**, *15*, 4903. [[CrossRef](#)] [[PubMed](#)]
48. Wang, S.; Liao, H.; Chen, Y.; Fernández-Steeger, T.M.; Du, X.; Xiong, M.; Liao, S. Damage evolution constitutive behavior of rock in thermo-mechanical coupling processes. *Materials.* **2021**, *14*, 7840. [[CrossRef](#)]

Disclaimer/Publisher’s Note: The statements, opinions and data contained in all publications are solely those of the individual author(s) and contributor(s) and not of MDPI and/or the editor(s). MDPI and/or the editor(s) disclaim responsibility for any injury to people or property resulting from any ideas, methods, instructions or products referred to in the content.